View metadata, citation and similar papers at core.ac.uk

brought to you by CORE

provided by VU Research Portal

VU UNIVERSITEIT AMSTERDAM

# VU Research Portal

## The Epstein-barr virus-encoded G protein-coupled receptor BILF1 hetero-oligomerizes with human CXCR4, scavenges G[alpha]i protein Chris s and constitutively impairs CXCR4 functioning, under revision

Nijmeijer, S.; Leurs, R.; Smit, M.J.; Vischer, H.F.

***published in***
Journal of Biological Chemistry
2010

***DOI (link to publisher)***
10.1074/jbc.M110.115618

***document version***
Publisher's PDF, also known as Version of record

**Link to publication in VU Research Portal**

***citation for published version (APA)***
Nijmeijer, S., Leurs, R., Smit, M. J., & Vischer, H. F. (2010). The Epstein-barr virus-encoded G protein-coupled receptor BILF1 hetero-oligomerizes with human CXCR4, scavenges G[alpha]i protein Chris s and constitutively impairs CXCR4 functioning, under revision. *Journal of Biological Chemistry*, *285*, 29632-29641. https://doi.org/10.1074/jbc.M110.115618

**General rights**
Copyright and moral rights for the publications made accessible in the public portal are retained by the authors and/or other copyright owners and it is a condition of accessing publications that users recognise and abide by the legal requirements associated with these rights.

- Users may download and print one copy of any publication from the public portal for the purpose of private study or research.
- You may not further distribute the material or use it for any profit-making activity or commercial gain
- You may freely distribute the URL identifying the publication in the public portal ?

**Take down policy**
If you believe that this document breaches copyright please contact us providing details, and we will remove access to the work immediately and investigate your claim.

**E-mail address:**
**vuresearchportal.ub@vu.nl**

Download date: 23. May. 2021

Supplemental Material can be found at:
http://www.jbc.org/content/suppl/2010/07/09/M110.115618.DC1.html

THE JOURNAL OF BIOLOGICAL CHEMISTRY VOL. 285, NO. 38, pp. 29632–29641, September 17, 2010
© 2010 by The American Society for Biochemistry and Molecular Biology, Inc. Printed in the U.S.A.

# The Epstein-Barr Virus-encoded G Protein-coupled Receptor BILF1 Hetero-oligomerizes with Human CXCR4, Scavenges $G\alpha_i$ Proteins, and Constitutively Impairs CXCR4 Functioning*[S]

Received for publication, February 18, 2010, and in revised form, July 8, 2010 Published, JBC Papers in Press, July 9, 2010, DOI 10.1074/jbc.M110.115618

**Saskia Nijmeijer, Rob Leurs, Martine J. Smit, and Henry F. Vischer**[1]

*From the Leiden/Amsterdam Center for Drug Research (LACDR), Division of Medicinal Chemistry, Faculty of Sciences, VU University Amsterdam, De Boelelaan 1083, 1081 HV Amsterdam, The Netherlands*

**Cells express distinct G protein-coupled receptor (GPCR) subtypes on their surface, allowing them to react to a corresponding variety of extracellular stimuli. Cross-regulation between different ligand-GPCR pairs is essential to generate appropriate physiological responses. GPCRs can physically affect each other's functioning by forming heteromeric complexes, whereas cross-regulation between activated GPCRs also occurs through integration of shared intracellular signaling networks. Human herpesviruses utilize virally encoded GPCRs to hijack cellular signaling networks for their own benefit. Previously, we demonstrated that the Epstein-Barr virus-encoded GPCR BILF1 forms heterodimeric complexes with human chemokine receptors. Using a combination of bimolecular complementation and bioluminescence resonance energy transfer approaches, we now show the formation of hetero-oligomeric complexes between this viral GPCR and human CXCR4. BILF1 impaired CXCL12 binding to CXCR4 and, consequently, also CXCL12-induced signaling. In contrast, the G protein uncoupled mutant BILF1-$K^{3.50}$A affected CXCL12-induced CXCR4 signaling to a much lesser extent, indicating that BILF1-mediated CXCR4 inhibition is a consequence of its constitutive activity. Co-expression of $G\alpha_{i1}$ with BILF1 and CXCR4 restored CXCL12-induced signaling. Likewise, BILF1 formed heteromers with the human histamine $H_4$ receptor ($H_4R$). BILF1 inhibited histamine-induced $G\alpha_i$-mediated signaling by $H_4R$, however, without affecting histamine binding to this receptor. These data indicate that functional cross-regulation of $G\alpha_i$-coupled GPCRs by BILF1 is at the level of G proteins, even though these GPCRs are assembled in hetero-oligomeric complexes.**

G protein-coupled receptors (GPCRs)[2] are integral membrane proteins that play a predominant role in sensory transduction and communication between cells. Specific binding of an extracellular messenger molecule (*i.e.* ligand) induces a conformational change in the GPCR protein, which allows intracellular coupling and activation of G proteins (1). These G proteins relay the message to downstream effector enzymes resulting in the activation of a broad range of cellular responses. The human genome encodes ~800 different GPCRs that are responsive to a plethora of endogenous (*e.g.* ions, lipid mediators, biogenic amines, amino acid, peptides, and glycoproteins) and exogenous (*e.g.* odorants, tastants, and light) ligands (2). Not surprisingly, GPCRs regulate nearly all physiological processes in our body. Most cells express 5–20 different GPCRs, which can be mixed and matched variably in different cell types (3). Cell type-specific GPCR expression profiles determine the spatiotemporal responsiveness of these cells to ligands in the extracellular environment.

GPCRs have long been considered to exist and function as monomeric proteins. However, during the last decade increasing evidence has indicated that GPCRs can interact physically with each other. In fact, the class C GPCR, $GABA_B$ receptor, and the sweet and umami taste receptors, TLR1–3, are obligatory heterodimers. Importantly, heteromerization of GPCR subtypes allows mutual regulation of the functional characteristics of the individual partners, including receptor trafficking, ligand binding, and receptor coupling to intracellular signaling pathways (4). Hitherto, understanding of the molecular mechanism of GPCR heteromers in relation to the recruitment of intracellular signaling complexes is still limited and sometimes even contradictory. Given the dimension of a GPCR in comparison to G protein and $\beta$-arrestin, it has been suggested that a GPCR dimer might provide the most appropriate docking surface for heterotrimeric G protein or $\beta$-arrestin coupling (5). Indeed, the human leukotriene $B_4$ receptor BLT1 was shown to exist as a pentameric complex consisting of a BLT1 homodimer and one heterotrimeric G protein (6). Nonetheless, only one of the two BLT1 protomers within this receptor dimer complex needs to be active to induce G protein coupling (7). Similar asymmetry in receptor activity has been observed within various other homo- and heterodimeric receptor complexes (8–10). Both rhodopsin and $\beta_2$-adrenergic receptors are organized as homodimers

* This work was supported by Veni Grant 700.55.403 (to H. F. V.) and Vidi Grant 700.54.425 (to M. J. S.) from the Netherlands Organization for Scientific Research and by Breakthrough Grant 93518006 from the Netherlands Genomics Initiative (to H. F. V.) and COST Action BM0806 (to S. N. and R. L.).

[S] The on-line version of this article (available at http://www.jbc.org) contains supplemental "Methods" and Figs. I–V.

[1] To whom correspondence should be addressed. Tel.: 31-20-5987588; Fax: 31-20-5987610; E-mail: vischer@few.vu.nl.

[2] The abbreviations used are: GPCR, G protein-coupled receptor; $H_4R$, histamine $H_4$ receptor; EBV, Epstein-Barr virus; BiLC, bimolecular luminescence complementation; BiFC, bimolecular fluorescence complementation; BRET, bioluminescence resonance energy transfer; TMR, tetramethylrhodamine; αBTX, α-bungarotoxin; BSA, bovine serum albumin; BBS, αBTX-binding site; CREB, cyclic AMP-responsive element-binding protein; FSK, forskolin; MOR, μ-opioid receptor; $\alpha_{2A}$-AR, $\alpha_{2A}$-adrenergic receptor; RSE, receptor surface expression; ANOVA, analysis of variance; GTPγS, guanosine 5′-3-*O*-(thio)triphosphate; eYFP, enhanced yellow fluorescent protein.

Downloaded from www.jbc.org at Vrije Universiteit, Medical Library, on December 21, 2011

(11, 12). However, reconstitution of rhodopsin and $\beta_2$-adrenergic receptor monomers in high density lipoprotein particles does not impair their capacity to activate G proteins (13, 14). In addition, the neurotensin receptor NTS1 activates G proteins more efficiently as a monomer than as a homodimer (15).

In addition, or alternatively, to cross-modulation of agonist-induced signaling within GPCR dimers, activation of one GPCR subtype can affect the functioning of co-expressed GPCRs through downstream cross-talk of their intracellular signaling pathways (16–18) and/or heterologous desensitization (19).

Human $\beta$- and $\gamma$-herpesviruses have one or more genes encoding for GPCR proteins that are expressed on the membrane of human cells upon viral infection (20). Recently, we demonstrated that the Epstein-Barr virus (EBV)-encoded GPCR BILF1 can form heterodimers with human chemokine receptors (21).

In the current study we further explore the interaction between BILF1 and the human chemokine receptor CXCR4. Using bimolecular luminescence complementation (BiLC) and bimolecular fluorescence complementation (BiFC) in tandem with bioluminescence resonance energy transfer (BRET) detection, we demonstrate that the orphan receptor BILF1 forms higher order hetero-oligomers with CXCR4. In addition, we show that BILF1 impairs binding of the chemokine CXCL12 to CXCR4 in a ligand-independent (constitutive) manner and, consequently, attenuates CXCL12-induced CXCR4 signaling.

## EXPERIMENTAL PROCEDURES

*Materials*—Cell culture media, trypsin, and accutase were obtained from PAA Laboratories (Pasching, Austria). Forskolin, pertussis toxin, and $\alpha$-bungarotoxin-tetramethylrhodamine (TMR-$\alpha$BTX) were purchased from Sigma-Aldrich. Penicillin and streptomycin were obtained from Lonza (Verviers, Belgium). Fetal bovine serum was purchased from Integro BV (Dieren, The Netherlands). HEPES and D-luciferin were purchased from Duchefa Biochemie (Haarlem, The Netherlands). Bovine serum albumin fraction V (BSA) was obtained from Roche Applied Science. [$^{125}$I]$\alpha$-Bungarotoxin ($\alpha$BTX; 2200 Ci/mmol), [$^{125}$I]CXCL12 (2200 Ci/mmol), [$^{3}$H]histamine (18.1 Ci/mmol), and [$^{35}$S]GTP$\gamma$S (1250 Ci/mmol) were obtained from PerkinElmer Life Sciences. CXCL12 was purchased from PeproTech (Rocky Hill, NJ), and Vectashield Hardset mounting medium was obtained from Vector Laboratories.

*Plasmids*—DNA plasmids encoding the full-length and complementation protein fragments of mVenus and Rluc8 were kindly provided by Dr. J. A. Javitch (Columbia University, New York) (22). To facilitate subcloning, the 5′-end of the original 24-amino acid N-terminal linker sequence of these constructs was substituted with SpeI/NotI restriction endonuclease sites by PCR, whereas the XhoI/XbaI sites were introduced immediately downstream of the stop codon. FLAG-BILF1, BBS-BILF1, BBS-BILF1-Rluc, and CXCR4-eYFP constructs have been described previously (21). Fusion of the 13-amino acid $\alpha$BTX-binding site (BBS) to the N terminus of BILF1 allows detection of receptor proteins by high affinity binding of TMR-$\alpha$BTX or [$^{125}$I]$\alpha$BTX. Rluc- and eYFP-encoding sequences were substituted with the DNA sequence of the full-length and complementation protein fragments of Rluc8 and mVenus using NotI and XbaI. The BILF1-K$^{3.50}$A construct was kindly provided by Dr. P. Beisser (Maastricht University Medical Center, The Netherlands). The K$^{3.50}$A mutation was subcloned into BBS-BILF1/pcDEF3 by using Psp5II and Van9II. All constructs were verified by DNA sequencing. DNA encoding the GABA$_{B2}$-YFP fusion protein was a gift from Dr. J.-P. Pin (Institut de Génomique Fonctionnelle, Montpellier, France). Myc-tagged human histamine $H_4$ receptor (myc-$H_4$R) has been described previously (23). The cyclic AMP-responsive element-binding protein (CREB)-driven luciferase reporter gene plasmid pTLNC-21CRE was provided by Dr. W. Born (National Jewish Medical and Research Center, Denver, CO). The cDNA clone for human G$\alpha_{i1}$ was obtained from the Missouri S&T cDNA Resource Center.

*Cell Culture and Transfection*—HEK293T cells were cultured and transiently transfected with the indicated amounts of DNA using 25-kDa linear polyethylenimine (Polysciences) as described previously (21). Total DNA in gene dosing experiments was kept constant by the addition of "empty" pcDEF3 plasmid.

*Protein Fragment Complementation and BRET*—HEK293T cells were cultured and transfected in white-bottomed 96-well plates. BiFC and BiLC were monitored 48 h after transfection as fluorescence (excitation at 498 nm and emission at 535 nm; 1-s recording) and luminescence in the presence of 5 $\mu$M coelenterazine H (emission at 460 nm; 1-s recording at 5 min after the addition of coelenterazine H (Promega)), respectively, using a Victor$^3$ 1420 multilabel plate reader (PerkinElmer Life Sciences). BRET was measured as described previously (21).

*BiFC Microscopy*—HEK23T cells were cultured and transfected in 10-cm dishes. Twenty-four hours after transfection cells were seeded on poly-L-lysine-coated coverslips in 6-well plates. The next day, coverslips were labeled with 0.6 $\mu$M TMR-$\alpha$BTX in phosphate-buffered saline for 30 min at room temperature. Coverslips were then washed twice with phosphate-buffered saline and once with $H_2O$. To stain cell nuclei, 4′, 6-diamidino-2-phenylindole (1 $\mu$g/$\mu$l) was added during the last wash step. Coverslips were placed on a microscope slide with one drop of Vectashield Hardset mounting medium and stored at 4 °C until further analysis. Cells were visualized using an Olympus FSX100 fluorescence microscope.

*Enzyme-linked Immunosorbent Assay (ELISA)*—Forty-eight hours after transfection, protein expression was determined by ELISA as described previously (24), with some minor changes. Cells were incubated with the anti-CXCR4 monoclonal IgG$_{2a}$ antibody, 12G5 (fusin) (1:800 dilution, 200 $\mu$g/$\mu$l, Santa Cruz Biotechnology). As secondary antibody, horseradish peroxidase-conjugated goat anti-mouse antibodies (1:2000 dilution, Bio-Rad) were used. Peroxidase activity was visualized using the 3,3′,5,5′-tetramethylbenzidine liquid substrate system (Sigma-Aldrich).

*Radioligand Binding*—Whole cell binding was performed 48 h after transfection using ~0.25 nM [$^{125}$I]$\alpha$BTX as described (21). Alternatively, cell membrane fractions from HEK293T cells expressing CXCR4, BBS-BILF1, and/or BBS-BILF1-K$^{3.50}$A were prepared as described previously (24). Cell membranes were incubated in 96-well plates in binding buffer (50 mM HEPES, 1 mM $CaCl_2$, 5 mM $MgCl_2$, and 100 mM NaCl, pH 7.4)

Downloaded from www.jbc.org at Vrije Universiteit, Medical Library, on December 21, 2011

containing 0.2% BSA with ~0.25 nM [$^{125}$I]αBTX or 0.08 nM [$^{125}$I]CXCL12 for 2 h at room temperature. Aspecific radioligand binding was determined in the presence of 0.1 μM unlabeled αBTX or CXCL12, respectively. Incubations were terminated by filtration through Unifilter GF/C plates (PerkinElmer Life Sciences) presoaked in 0.3% polyethylenimine and washed three times with ice-cold binding buffer supplemented with 0.5 M NaCl. Radioactivity was measured using a MicroBeta Trilux (PerkinElmer Life Sciences).

*[$^{35}$S]GTPγS Binding*—Cell membranes were incubated in 96-well plates in assay buffer (50 mM HEPES, 10 mM $MgCl_2$, and 100 mM NaCl, pH 7.2), 5 μg of saponin, 3 μM GDP, and 0.5 nM [$^{35}$S]GTPγS, in the absence or presence of 100 nM CXCL12, in a total volume of 100 μl. Reactions were incubated at room temperature for 1 h and then terminated by filtration through Unifilter GF/B plates (PerkinElmer Life Sciences) and washed three times with ice-cold washing buffer (50 mM Tris-HCl and 5 mM $MgCl_2$, pH 7.4). Radioactivity was measured using a Microbeta Trilux.

*CREB Reporter Gene Assay*—HEK293T were cultured in white-bottomed 96-well plates and co-transfected with 500 ng of reporter gene plasmid, pTLNC-21CRE (consisting of a firefly luciferase gene controlled by a 21-cAMP-responsive element-containing promoter) and 10–50 ng of CXCR4, BBS-BILF1, and/or BBS-BILF1-K$^{3.50}$A DNA/10$^6$ cells. Forty-eight hours after transfection, the culture medium was aspirated, and cells were stimulated with 100 nM CXCL12 in culture medium supplemented with 1 μM forskolin for 6 h at 37 °C. Luciferase activity was measured as described previously (25).

*Data Analysis*—All experiments were repeated using cells from independent transfections. Curve fitting and statistical analyses were performed using GraphPad Prism 4 software.

## RESULTS

*BILF1 Forms Higher Order Hetero-oligomers with CXCR4*—The optimized BRET sensors Rluc8 (26) and mVenus (27) were used to show close proximity between BILF1 and CXCR4. Bioluminescence and fluorescence emitted by GPCR-BRET sensor constructs increased linearly with increasing receptor numbers (data not shown), confirming previous observations (28, 29). BBS-BILF1 expression was determined by [$^{125}$I]αBTX binding, whereas expression of CXCR4 constructs was quantified by ELISA. Both BBS-BILF1-Rluc8 and CXCR4-Rluc8 emitted significantly ($p < 0.0001$) more light per receptor number than the previously described BBS-BILF1-Rluc and CXCR4-Rluc, respectively (Fig. 1*A*) (21). On the other hand, the mVenus variants of BILF1 and CXCR4 were less or equally fluorescent per receptor, respectively, as compared with their previously used eYFP counterparts (Fig. 1*B*) (21). BRET experiments were performed using these optimized BRET sensor constructs by transfecting 1 ng of receptor-Rluc8 (donor) DNA in combination with 0–1000 ng of receptor-mVenus (acceptor) DNA/10$^6$ cells. Saturable BRET signals indicate specific interactions between BILF1-BILF1, BILF1-CXCR4, and CXCR4-CXCR4 BRET pairs, which is consistent with our previous work (21) (Fig. 1, *C* and *D*). Typically, BRET signals were higher for both BILF1 and CXCR4 homodimers as compared with BILF1-CXCR4 heterodimers. The latter was independent of the BRET sensor orientation, as swapping the sensors between BILF1 and CXCR4 yielded a similar BRET signal for the heterodimeric interaction. Nonspecific receptor interactions as a consequence of random collisions were observed as quasi-linear BRET signals in cells co-expressing BBS-BILF1-Rluc8 or CXCR4-Rluc8 with $GABA_{B2}$-YFP (Fig. 1, *C* and *D*).

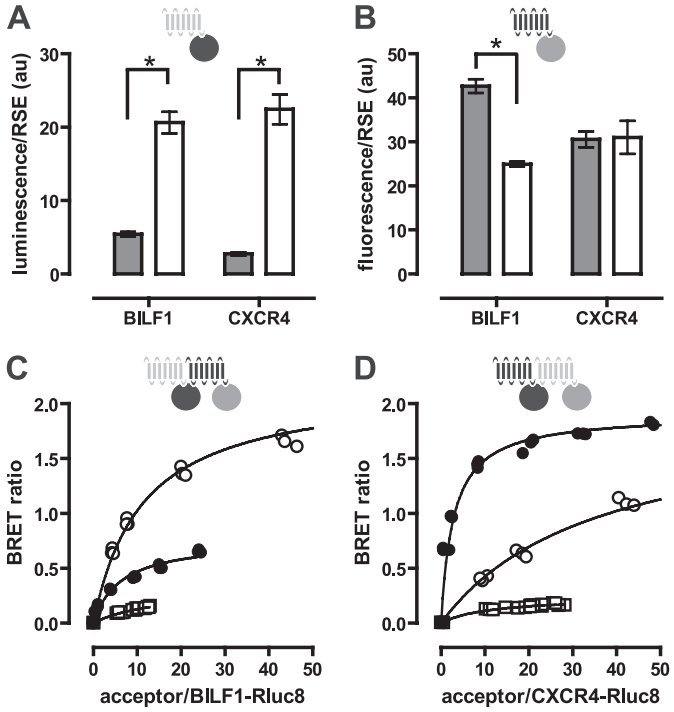


FIGURE 1. **Detection of BILF1 and CXCR4 heterodimers by BRET.** *A* and *B*, HEK293T cells were transfected with BBS-BILF1 or CXCR4 BRET fusion constructs. After 48 h, receptor surface expression (RSE) levels were quantified for BBS-BILF1 and CXCR4 by [$^{125}$I]αBTX binding or ELISA, respectively, on whole cells. Measured Rluc (*gray bars*) and Rluc8 (*white bars*) luminescence (*A*) and eYFP (*gray bars*) and mVenus (*white bars*) fluorescence (*B*) are normalized for RSE. *C* and *D*, HEK293T cells were transfected with fixed amounts of the BRET donor construct BBS-BILF1-Rluc8 (*C*) and CXCR4-Rluc8 (*D*) DNA and increasing amounts of BRET acceptor constructs BBS-BILF1-mVenus (○), CXCR4-mVenus (●), and $GABA_{B2}$-YFP (□) DNA. The BRET ratio is defined as [BRET/luminescence] in the presence of acceptor constructs minus [BRET/luminescence] in the absence of acceptor constructs. BRET ratio was plotted as a function of the increasing acceptor/donor ratio as quantified by fluorescence and luminescence, respectively. Data are means ± S.E. of representative experiments performed at least three times in triplicate. Significant differences ($p < 0.0001$) were determined using a *t* test and are indicated by *asterisks*. Curves were fitted using nonlinear regression, assuming a single binding site. *au*, arbitrary units.

To study higher order protein-protein interactions in living cells, we used BiLC and BiFC approaches in combination with BRET. N- and C-terminal complementation fragments of the optimized BRET couple Rluc8 and mVenus have been developed by the Javitch laboratory (22). Rluc8 was split into L1 (amino acids 1–229) and L2 (amino acids 230–311), whereas mVenus was split in V1 (amino acids 1–155) and V2 (amino acids 156–240). Expression of the individual receptor-L1, -L2, -V1, and -V2 fusion constructs in HEK293T cells did not significantly increase luminescence or fluorescence above background (data not shown), confirming previous observations (22). Co-expression of BBS-BILF1-L1 with CXCR4-L2 or CXCR4-L1 with BBS-BILF1-L2 resulted in BiLC (Fig. 2, *A* and *B*). Functional reconstitution of the Rluc8 protein occurred only when the L1 and L2 fragments were brought into close

Downloaded from www.jbc.org at Vrije Universiteit, Medical Library, on December 21, 2011

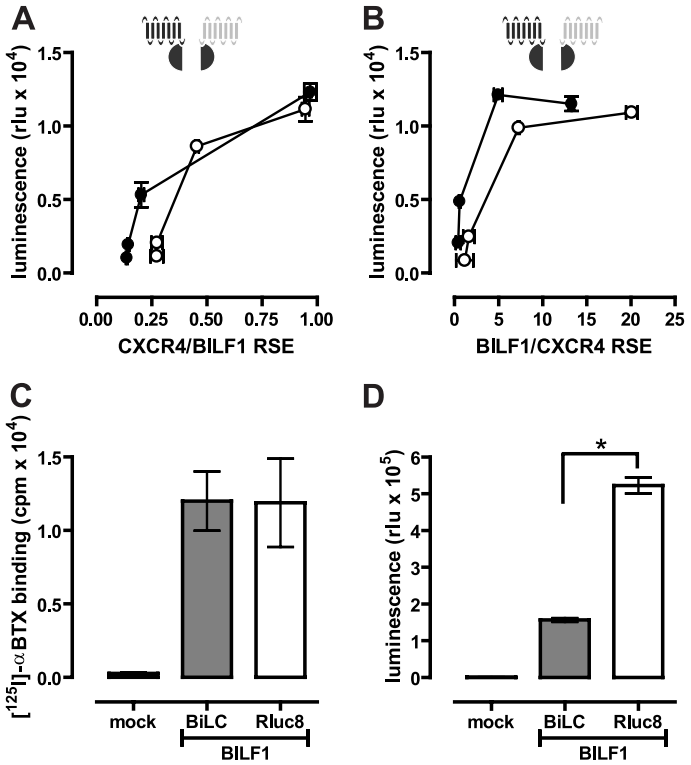


FIGURE 2. **Detection of BILF1 and CXCR4 heterodimers by BiLC and BiFC.** *A*, HEK293T cells were co-transfected with 10 ng of BBS-BILF1-L1 and 1–50 ng of CXCR4-L2 DNA/$10^6$ cells (○) or 10 ng of BBS-BILF1-L2 and 1–50 ng of CXCR4-L1 (●). *B*, HEK293T cells were co-transfected with 10 ng of CXCR4-L1 and 1–50 ng of BBS-BILF1-L2 (○) or 10 ng of CXCR4-L2 and 1–50 ng of BBS-BILF1-L1 (●). Luminescence was measured after 48 h and plotted as a function of BBS-BILF1 and CXCR4 RSE as determined by [$^{125}$I]αBTX binding and ELISA, respectively. *C* and *D*, HEK293T cells were co-transfected with the split BiLC constructs BBS-BILF1-L1 and BBS-BILF1-L2 or BBS-BILF1-Rluc8. The RSE of the BBS-BILF1 fusion proteins was determined by [$^{125}$I]αBTX binding (*C*), and luminescence was measured in parallel (*D*). *E–H*, HEK293T cells were co-transfected with 10 ng of BBS-BILF1-V1 and CXCR4-V2 DNA/$10^6$ cells and cultured on poly-L-lysine-coated coverslips. After 48 h, the BBS-BILF1 protomer was labeled with TMR-αBTX as depicted in the schematic (*E*). Reconstituted mVenus (*green* (*F*)), TMR-αBTX labeling (*red* (*G*)), and co-localization (*yellow* (*H*)) were analyzed using an Olympus FSX100 fluorescence microscope. Nuclei were stained with 4′,6-diamidino-2-phenylindole (*blue*). Data are means ± S.E. of representative experiments performed at least three times in triplicate. *rlu*, relative light units.

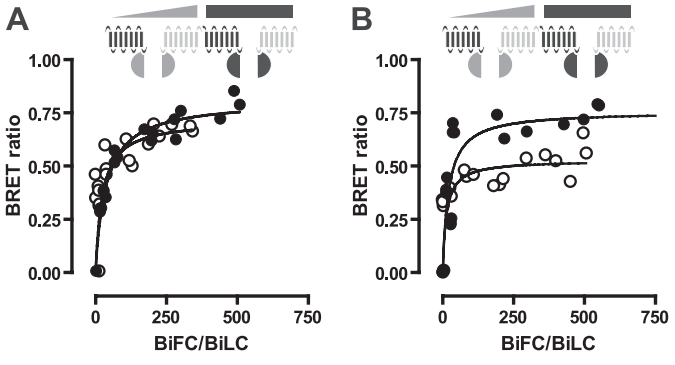


FIGURE 3. **Detection of BILF1 and CXCR4 hetero-oligomers by BiLC/BiFC-BRET.** *A*, HEK293T cells were co-transfected with 10 ng of DNA from the BiLC constructs BBS-BILF1-L1 and CXCR4-L2 (1:1) and 0–950 ng of DNA from the BiFC constructs BBS-BILF1-V1 and CXCR4-V2 (○) or CXCR4-V1 and BBS-BILF1-V2 (●) (1:1)/$10^6$ cells. *B*, BiLC constructs CXCR4-L1 and BBS-BILF1-L2 in combination with BiFC constructs BBS-BILF1-V1 and CXCR4-V2 (○) or CXCR4-V1 and BBS-BILF1-V2 (●). After 48 h, fluorescence, luminescence, and BRET were measured. The BRET ratio was plotted as a function of the increasing reconstituted acceptor (BiFC)/donor (BiLC) ratio as quantified by fluorescence and luminescence, respectively. Data are representative of at least three independent experiments each performed in triplicate.

proximity by the proteins to which they were fused, confirming that BILF1 and CXCR4 form heterodimers. Co-expression of BBS-BILF1-L1 and BBS-BILF1-L2 in a 1:1 ratio at a total receptor surface level equal to that of BBS-BILF1-Rluc8 (Fig. 2*C*) yielded a 3.3-fold lower BiLC signal compared with BBS-BILF1-Rluc8 luminescence (Fig. 2*D*). Considering that three populations of BILF1 homodimers exist in cells co-expressing BBS-BILF1-L1 and BBS-BILF1-L2 (*i.e.* L1/L1, L1/L2, and L2/L2), the observed BiLC signal suggests that all BILF1 receptors are involved in dimers. Reconstitution of mVenus by BBS-BILF1-V1 and CXCR4-V2 and vice versa, in combination with the binding of TMR-αBTX to surface-expressed BILF1 (Fig. 2, *E–H*), revealed that BILF1-CXCR4 heterodimers are localized at the cell surface (Fig. 2*H*) confirming our previous findings (21). The punctuated *green* areas are newly formed intracellular BILF1/CXCR4 heterodimers, as indicated by the absence of co-localized TMR-αBTX fluorescence (Fig. 2, *F–H*). On the other hand, internalized receptor complexes are indicated by intracellularly localized TMR-αBTX-labeled BILF1/CXCR4 heterodimers. Higher order BILF1-CXCR4 protein complexes were detected by measuring BRET between reconstituted L1/L2 and V1/V2 heterodimers of BILF1 and CXCR4. To this end, cells were co-transfected with constant amounts of the split Rluc8 constructs (*i.e.* 10 ng of both L1 and L2 construct DNA/$10^6$ cells) with increasing amounts of the split mVenus constructs (*i.e.* 0–950 ng of both V1 and V2 construct DNA/$10^6$ cells). A saturable BRET signal was observed between all combinations of complemented Rluc8 and mVenus, indicating that BILF1 and CXCR4 form oligomeric complexes consisting of at least four protomers (Fig. 3).

*Constitutively Active BILF1 Inhibits CXCL12 Binding to CXCR4*—To investigate whether hetero-oligomerization of BILF1 and CXCR4 affects chemokine (*i.e.* CXCL12) binding to the latter, BBS-BILF1 (2.5 or 25 ng DNA/$10^6$ cells) and CXCR4 (50 ng DNA/$10^6$ cells) were co-expressed in HEK293T cells. Radioligand binding assays were performed on membrane fractions expressing individual or both receptors. CXCR4 expression was evaluated by ELISA on whole cells of the same transfection. BBS-BILF1 significantly impaired binding of CXCL12 to CXCR4 in an expression level-dependent manner, without having a major effect on CXCR4 protein levels (Fig. 4). The slight reduction in CXCR4 protein expression at 25 ng of BILF1

Downloaded from www.jbc.org at Vrije Universiteit, Medical Library, on December 21, 2011

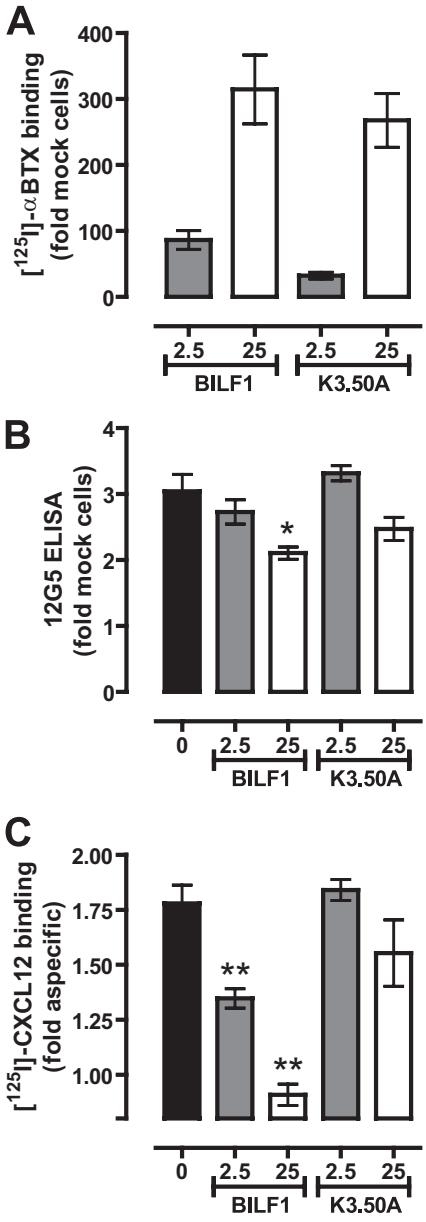


FIGURE 4. **BILF1 inhibits CXCL12 binding to CXCR4.** HEK293T cells were co-transfected with 50 ng of CXCR4 and 0, 2.5 or 25 ng of BBS-BILF1 or BBS-BILF1-$K^{3.50}$A DNA/$10^6$ cells. *A*, DNA dose-dependent BBS-BILF1 and BBS-BILF1-$K^{3.50}$A expression was shown by [$^{125}$I]αBTX binding to membrane preparations. *B*, CXCR4 expression was determined in parallel by ELISA. *C*, [$^{125}$I]CXCL12 binding on the same membrane set. Data are means ± S.E. from three independent experiments, each performed in triplicate. Statistical differences between CXCR4 in the absence or presence of BBS-BILF1-($K^{3.50}$A) were determined using a one-way ANOVA followed by a Bonferroni's multiple comparison test (*, $p < 0.05$; **, $p < 0.001$).

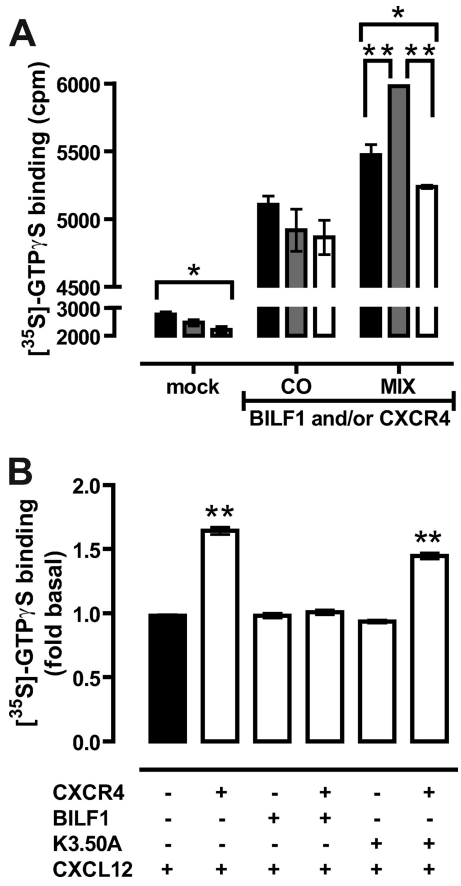


FIGURE 5. **BILF1 inhibits CXCL12-induced G protein activation by CXCR4.** HEK293T cells were transfected with 50 ng of CXCR4 and/or 20 ng of BBS-BILF1 DNA or BBS-BILF1-$K^{3.50}$A DNA/$10^6$ cells. *A*, CXCL12-induced (0.1 μM) binding of [$^{35}$S]GTPγS was measured in membranes derived from cells co-transfected with BBS-BILF1 and CXCR4 (*CO*) or from cells expressing either BBS-BILF1 or CXCR4 that were mixed prior to membrane preparation (*MIX*) in response to a 1-h incubation with buffer (*black bars*), 0.1 μM CXCL12 (*gray bars*), or 0.1 μM CXCL12 and 10 μM AMD3100 (*white bars*). Mock-transfected cells were used as control. *B*, binding of [$^{35}$S]GTPγS to membranes expressing the indicated receptor constructs was determined in response to vehicle treatment or 0.1 μM CXCL12. To emphasize changes in ligand-induced signaling, [$^{35}$S]GTPγS binding was normalized to vehicle treatment for each of the membrane preparations and consequently is shown as fold basal. Data are means ± S.E. from three independent experiments, each performed in triplicate. Statistical differences were determined using a one-way ANOVA followed by a Bonferroni's multiple comparison test (*, $p < 0.05$; **, $p < 0.001$).

DNA transfection was not the cause of the loss of CXCL12 binding (Fig. 4, *B* and *C*), as individually expressed CXCR4 at comparable levels still bound CXCL12 (supplemental Fig. I). To determine whether the constitutive activity of BILF1 hampers CXCL12 binding to CXCR4 by, for example, inducing a cross-conformational change in the assembled CXCR4 protomer, similar binding experiments were performed on membranes co-expressing the constitutively inactive mutant BBS-BILF1-$K^{3.50}$A (30). BILF1-$K^{3.50}$A has a propensity similar to BILF1 to heterodimerize with CXCR4 (supplemental Fig. II). BBS-BILF1-$K^{3.50}$A was co-expressed with CXCR4 at levels comparable to that of BILF1 (Fig. 4*A*). Similar to BILF1, the transfection of 25 ng of BBS-BILF1-$K^{3.50}$A DNA/$10^6$ cells resulted in a slight reduction of CXCR4 expression as measured with the anti-CXCR4 antibody 12G5 (Fig. 4*B*). However, BBS-BILF1-$K^{3.50}$A had no significant effect on CXCL12 binding to membranes co-expressing CXCR4, as compared with membranes expressing only CXCR4 (Fig. 4*C*).

*Constitutively Active BBS-BILF1 Inhibits CXCL12-induced CXCR4 Signaling through $G\alpha_{i/o}$ Proteins*—To evaluate the effect of BBS-BILF1 co-expression on CXCR4-mediated G protein activation, [$^{35}$S]GTPγS binding to membranes expressing both receptors was measured and compared with membranes that were derived from HEK293T cells that express either BBS-BILF1 or CXCR4 and were mixed in an 1:1 ratio (Fig. 5*A*). Constitutive binding of [$^{35}$S]GTPγS was observed in both co-expressing and mixed membranes as a result of constitutive

Downloaded from www.jbc.org at Vrije Universiteit, Medical Library, on December 21, 2011

signaling of BBS-BILF1 (Fig. 5*A* and supplemental Fig. III). Subsequent stimulation of membranes co-expressing BBS-BILF1 and CXCR4 with 0.1 $\mu$M CXCL12 did not increase basal [$^{35}$S]GTP$\gamma$S binding (Fig. 5, *A* and *B*). In contrast, CXCL12 significantly increased [$^{35}$S]GTP$\gamma$S binding to mixed membranes, which can be fully blocked by the CXCR4 antagonist AMD3100 (10 $\mu$M) (Fig. 5*A*). CXCL12 induced a significant 1.64-fold increase in [$^{35}$S]GTP$\gamma$S binding to CXCR4-expressing membranes as compared with vehicle treatment (Fig. 5*B*). In contrast, CXCL12 did not change [$^{35}$S]GTP$\gamma$S binding to mock, BBS-BILF1-, and BBS-BILF1-K$^{3.50}$A-expressing membranes differently from vehicle treatment (Fig. 5*B* and supplemental Fig. III). Interestingly, co-expression of the constitutively inactive mutant BBS-BILF1-K$^{3.50}$A with CXCR4 did not affect CXCL12-induced G protein activation, resulting in a similar increase in [$^{35}$S]GTP$\gamma$S binding as observed in membranes that express CXCR4 alone (Fig. 5*B* and supplemental Fig. III).

Both CXCR4 and BBS-BILF1 signal through G$\alpha_{i/o}$ proteins (25, 31, 32). To examine downstream signaling, HEK293T cells were co-transfected with a CREB-driven reporter gene plasmid and CXCR4 and/or BBS-BILF1. Receptor surface expression of CXCR4 was determined by ELISA. BBS-BILF1 slightly reduced CXCR4 expression levels (Fig. 6*A*). To detect G$\alpha_{i/o}$-mediated inhibitory signaling to CREB, intact cells were incubated with 1 $\mu$M forskolin (FSK) leading to a direct activation of adenylyl cyclase. Expression of BBS-BILF1 resulted in a ligand-independent decrease of this FSK-induced CREB activity (supplemental Fig. IV*A*) as shown previously (25, 32). Stimulation of CXCR4-expressing cells with 0.1 $\mu$M CXCL12 resulted in a significant decrease of FSK-induced CREB activity as compared with vehicle treatment (Fig. 6*B* and supplemental Fig. IV*B*). However, co-expression of the constitutively active BBS-BILF1 with CXCR4 significantly attenuated this CXCL12-induced inhibition of CREB activity (Fig. 6*B*). In contrast, the constitutively inactive mutant BBS-BILF1-K$^{3.50}$A inhibited CXCL12-induced CXCR4 signaling to a much lesser extent than BBS-BILF1. Overnight pretreatment of the cells with pertussis toxin (100 ng/$\mu$l) abolished all BBS-BILF1- and/or CXCR4-mediated inhibition of FSK-induced CREB activity (supplemental Fig. V), confirming signaling through G$\alpha_{i/o}$ proteins (25, 31, 32).

*Constitutively Active BBS-BILF1 Competes with Co-expressed GPCR for G$\alpha_{i/o}$ Proteins*—The difference in efficacy between the constitutively active BBS-BILF1 and constitutively inactive mutant BBS-BILF1-K$^{3.50}$A in regard to CXCR4 signaling might be related to the stabilization of distinct CXCR4 conformations in their respective hetero-oligomeric complexes, resulting in changed CXCL12 binding and, consequently, signaling. Alternatively, the constitutively active BBS-BILF1 might scavenge G$\alpha_{i/o}$ proteins to such an extent that only a very limited amount of G proteins are available for coupling to CXCR4. To evaluate the role of G protein coupling on CXCL12 binding to CXCR4, [$^{125}$I]CXCL12 binding experiments were performed in the presence of 3 $\mu$M GTP$\gamma$S. Binding of CXCL12 to CXCR4 was fully inhibited by preventing G protein coupling to the receptor (Fig. 7*A*). On the other hand, co-expression of additional G$\alpha_{i1}$ protein with CXCR4 and BBS-BILF1 restored CXCR4-mediated inhibition of CREB activity in response to

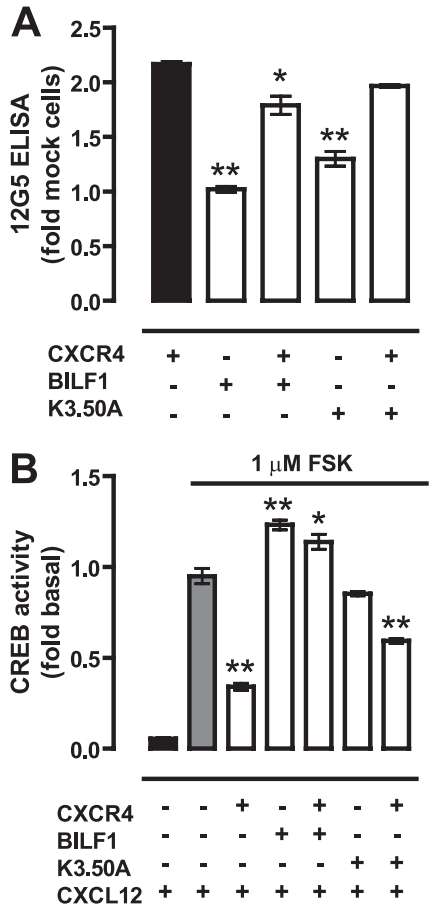


FIGURE 6. **BILF1 inhibits CREB activation by CXCR4 in response to CXCL12.** *A*, CXCR4 RSE in HEK293T cells transfected with CXCR4 (50 ng/10$^6$ cells), BBS-BILF1 (25 ng/10$^6$ cells), and/or BBS-BILF1-K$^{3.50}$A (25 ng/10$^6$ cells) as determined by ELISA. *B*, FSK-induced CREB activity was measured in parallel in the absence or presence of 0.1 $\mu$M CXCL12. To emphasize changes in ligand-induced signaling, CREB activity is normalized to vehicle treatment for each of the transfectants and consequently shown as fold basal. Data are means ± S.E. of representative experiments performed at least three times in triplicate. Significantly changes in CXCR4 RSE as compared with CXCR4-only cells are determined by a one-way ANOVA followed by a Bonferroni's multiple comparison test (*A*). Significant changes in CREB activity in the presence of CXCL12 as compared with mock cells were determined by the same statistical analysis (*, $p < 0.05$; **, $p < 0.001$).

CXCL12 (Fig. 7*B*) without significantly affecting receptor surface expression (Fig. 7*C*). To further explore whether constitutive BBS-BILF1 signaling affects the functioning of other GPCRs that couple to G$\alpha_{i/o}$ proteins, HEK293T cells were transfected with BBS-BILF1 or BBS-BILF1-K$^{3.50}$A and/or human $H_4$R. BBS-BILF1 and $H_4$R receptor were expressed at the cell surface and formed heterodimeric complexes as revealed by BiFC, although internalized TMR-$\alpha$BTX-labeled BBS-BILF1/$H_4$R heterodimers were observed as well (Fig. 8, *A–D*). Histamine (10 $\mu$M) significantly decreased FSK-induced CREB activity in HEK293T cells expressing $H_4$R, as compared with vehicle treatment, without affecting BBS-BILF1 signaling to CREB (Fig. 8*E*). Co-expression of BBS-BILF1 with $H_4$R abolished the histamine responsiveness of $H_4$R, whereas BBS-BILF1-K$^{3.50}$A did not disturb histamine-induced signaling to CREB (Fig. 8*E*). In contrast to [$^{125}$I]CXCL12 binding to CXCR4, [$^3$H]histamine binding to h$H_4$R-expressing membranes was not affected by BBS-BILF1 (Fig. 8*F*), which confirms that hista-

Downloaded from www.jbc.org at Vrije Universiteit, Medical Library, on December 21, 2011

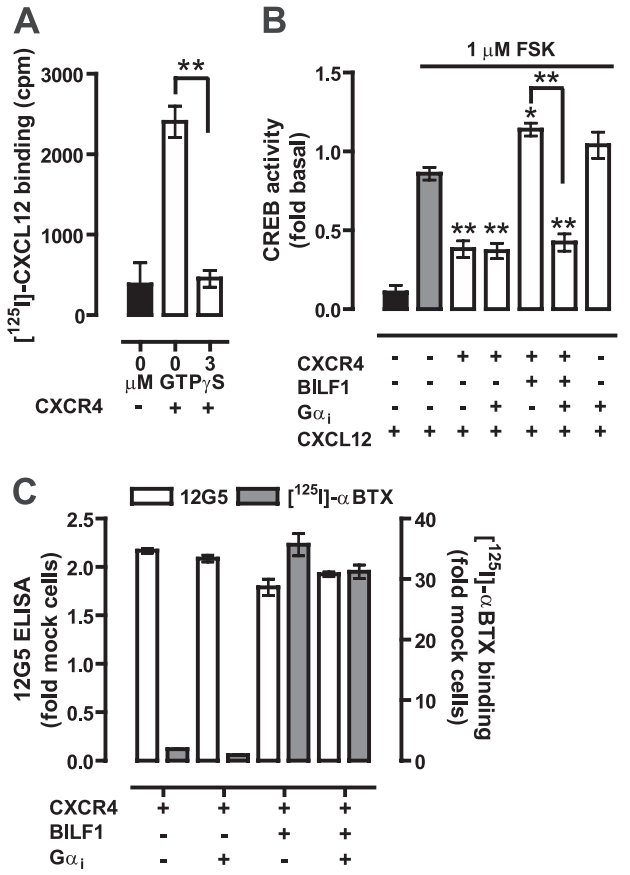


FIGURE 7. **BILF1 inhibits CXCL12-induced CXCR4 signaling by scavenging $G\alpha_i$ proteins.** *A*, [$^{125}$I]CXCL12 binding to CXCR4-expressing membranes in the absence and presence of 3 $\mu$M GTP$\gamma$S. *B*, FSK-induced CREB activity in cells expressing the indicated receptors in the absence or presence of co-transfected $G\alpha_{i1}$ proteins in response to vehicle or 0.1 $\mu$M CXCL12 treatment. CXCL12-modulated CREB activity is normalized to vehicle treatment for each of the transfectants and consequently shown as fold basal. *C*, BBS-BILF1 and CXCR4 RSE as determined by [$^{125}$I]$\alpha$BTX binding or ELISA to whole cells, respectively. Data are means ± S.E. of representative experiments performed at least three times in triplicate. Significant differences compared with FSK-treated mock cells (*gray bar* (*B*)), unless otherwise specified, are indicated by *asterisks* as determined using a one-way ANOVA followed by a Bonferroni's multiple comparison test (*, $p < 0.05$; **, $p < 0.001$).

mine binding to $H_4R$ is not affected by G protein uncoupling with GTP$\gamma$S (Fig. 8*G*) (33).

## DISCUSSION

EBV hides latently in memory B cells in ~95% of all human beings. Terminal differentiation of these infected memory B cells into antibody-secreting plasma cells reinitiates the replicative cycle of EBV, ultimately leading to the production of new infectious virions (34). One of the viral genes that is up-regulated during this replicative cycle is the EBV-encoded GPCR BILF1 (25, 32, 35). BILF1 constitutively signals to CREB and NF-$\kappa$B via pertussis toxin-sensitive $G_{i/o}$ protein-mediated pathways (25, 32), as corroborated in this study by, for example, the constitutive increase of GTP$\gamma$S binding to BILF1-expressing membranes.

Previously we showed that BILF1 forms heteromeric complexes with human chemokine receptors that are expressed endogenously on plasma B cells (21). However, the previously used time-resolved BRET and co-immunoprecipitation methods could not distinguish dimeric from oligomeric assemblages (21). By combining BiFC and BiLC with BRET measurements, we now showed that heteromeric complexes between BILF1 and CXCR4 consist of at least four interacting GPCR proteins at the same time. Such oligomeric organization has been observed for native rhodopsin in disc membranes of rod outer segments by using atomic force microscopy (11) but have also been observed between class C GPCRs $GABA_{B1}$ and $GABA_{B2}$ (36) and between various class A GPCRs using various modifications and/or combinations of resonance energy transfer-based methods as well as cross-linking experiments (22, 37–41). Hitherto, however, the functional significance and/or necessity of oligomeric receptor complexes *versus* receptor dimers have remained puzzling. For example, the dopamine D2 receptor is organized as homo-oligomers consisting of at least four receptors (22). However, co-expression of a non-signaling dopamine D2 receptor-G protein fusion construct with wild type dopamine D2 receptor revealed that a functional signaling complex consists of two GPCR protomers and a single heterotrimeric G protein (9). Moreover, dimerization of obligatory $GABA_B$ heterodimers attenuated G protein coupling in response to GABA as compared with signaling of individual $GABA_B$ heterodimers, suggesting that the level of oligomerization might control signaling efficacy (36).

Co-expression of BILF1 and CXCR4 in HEK293T cells impaired CXCL12 binding to CXCR4. Previously, CXCR4 was shown to heterodimerize with the chemokine receptors CCR2 (42), CCR5 (41), and CXCR7 (43). The chemokines CCL2 and CCL4 do not interact with CXCR4. However, CCL2 and CCL5 inhibit CXCL12 binding to CXCR4 upon co-expression of CCR2 and CCR5, respectively (41, 42). Likewise, CXCL12 inhibits CCL2 and CCL4 binding to cells co-expressing CCR2 or CCR5 with CXCR4. The observed negative binding cooperativity across these chemokine receptor heterodimers is the consequence of allosteric modulation of the ligand-binding site conformation of one protomer upon binding of a ligand to the other protomer, as revealed by a significant acceleration of radioligand dissociation from one protomer under infinite tracer dilution conditions in the presence of unlabeled chemokine or nonpeptidergic ligand of the second protomer (41, 42).

Such transmission of a conformational change across a receptor heterodimer was shown directly between the $\mu$-opioid receptor (MOR) and the $\alpha_{2A}$-adrenergic receptor ($\alpha_{2A}$-AR). Binding of morphine to MOR induces a conformational change in the norepinephrine-occupied $\alpha_{2A}$-AR, as detected by a change in norepinephrine-induced FRET between two fluophores incorporated into the C-tail and intracellular loop 3 of $\alpha_{2A}$-AR, respectively (10). As a consequence, norepinephrine-induced signaling of $\alpha_{2A}$-AR to G proteins is inhibited within milliseconds upon binding of morphine to MOR. In addition, simultaneous stimulation of these transfected cells or primary spinal cord neurons with MOR and $\alpha_{2A}$-AR agonists attenuates extracellular signal-regulated kinases 1 and 2 (ERK1/2) phosphorylation as compared with stimulation with either of these agonists (10) (44). Hence, the activation of one protomer by agonist binding is sufficient to induce signal transduction, whereas agonist occupancy of both protomers attenuates receptor dimer-mediated signaling. On the other hand, stabili-

Downloaded from www.jbc.org at Vrije Universiteit, Medical Library, on December 21, 2011

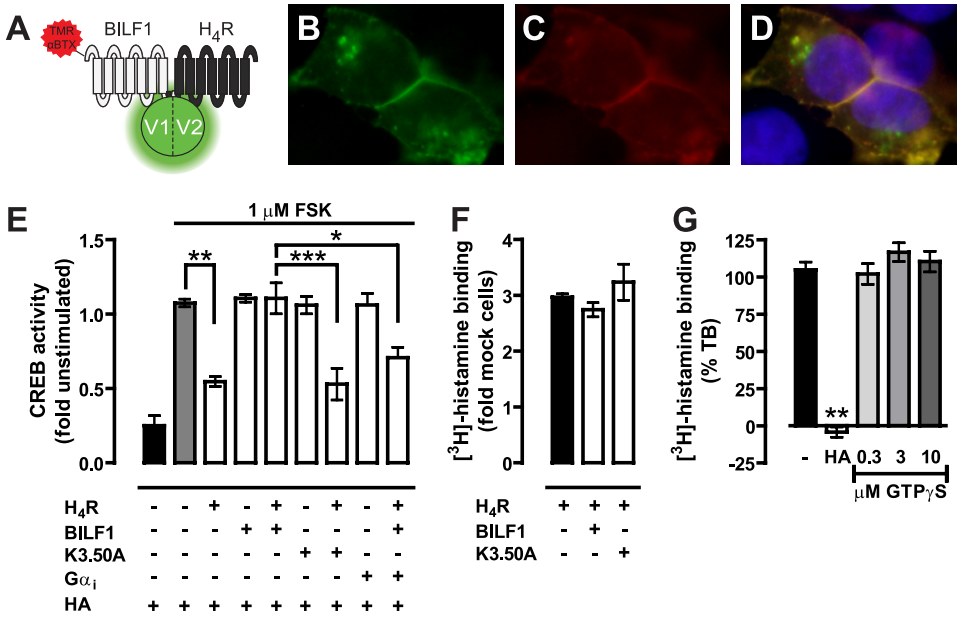


FIGURE 8. **BILF1 forms heteromers with $H_4R$ and inhibits histamine-induced signaling without affecting binding.** *A–D*, HEK293T cells were co-transfected with 50 ng of $H_4R$-V1 and BBS-BILF1-V2 DNA/$10^6$ cells and cultured on poly-L-lysine-coated coverslips. After 48 h, the BBS-BILF1 protomer was labeled with TMR-αBTX as depicted in the schematic (*A*), and co-localization (*yellow* (*D*)) of reconstituted mVenus (*green* (*B*)) and TMR-αBTX (*red* (*C*)) was analyzed using an Olympus FSX100 fluorescence microscope. Nuclei were stained with 4′,6-diamidino-2-phenylindole (*blue*). *E*, FSK-induced CREB activity in cells in the absence or presence of 10 μM histamine (*HA*) 48 h after transfection with 50 ng of Myc-$H_4R$ and/or 25 ng of BBS-BILF1 or BILF-$K^{3.50}$A DNA/$10^6$ cells. Histamine-induced CREB activity is normalized to vehicle treatment for each of the transfectants and consequently shown as fold basal. *F*, [$^3$H]histamine binding to membranes expressing the indicated receptors. *G*, [$^3$H]histamine binding to membranes expressing $H_4R$ in the presence of 10 μM histamine or increasing concentrations (0.3–10 μM) of GTPγS. The *bar graphs* represent the mean of pooled data from at least two experiments performed in triplicate. *Error bars* indicate S.E. Significant differences are indicated by *asterisks*, as determined using a one-way ANOVA followed by a Bonferroni's multiple comparison test (*, $p < 0.05$; **, $p < 0.01$; ***, $p < 0.001$).

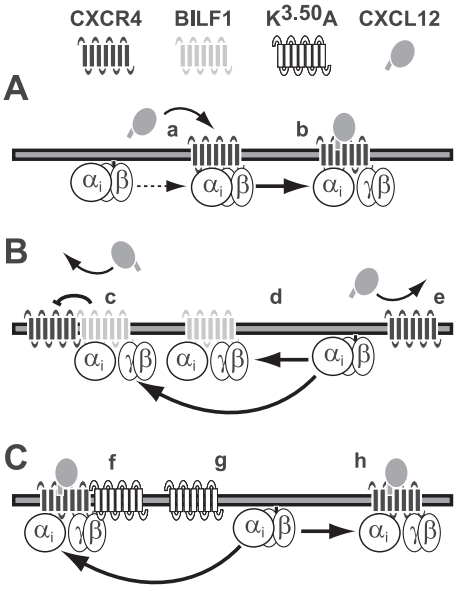


FIGURE 9. **Schematic representation of the inhibition of CXCR4 by the constitutively active BILF1.** *A*, CXCL12 binding to CXCR4 is $G\alpha_i$ protein-dependent (*a*) and results in receptor and G protein activation (*b*). *B*, constitutively active BILF1 heteromerizes with CXCR4 and may allosterically inhibit CXCL12 binding to CXCR4 (*c*). Moreover, BILF1 constitutively recruits and activates $G\alpha_i$ proteins (*d*). This scavenging prevents $G\alpha_i$ proteins from interacting with CXCR4, resulting in an inhibition of CXCL12 binding (*e*). *C*, the constitutively inactive mutant BILF1-$K^{3.50}$A is not able to cross-inhibit CXCL12 binding to CXCR4 upon heteromerization (*f*). BILF1-$K^{3.50}$A does not compete with CXCR4 for available $G\alpha_i$ proteins (*g*), allowing $G\alpha_i$ protein-dependent CXCL12 binding to CXCR4 (*h*). For the sake of clarity, receptor homomers and oligomers are not shown in this figure.

zation of the inactive conformation of one protomer with an inverse agonist results in an increase in agonist-induced signaling of the associated protomer (9). This indicates that a constitutively active protomer decreases agonist-induced signaling of the second protomer within the receptor dimer, which is in line with the observed decrease in responsiveness of CXCR4 to CXCL12 when co-expressed with the constitutively active BILF1. Because inverse agonists for BILF1 are yet to be identified, a constitutively inactive mutant of BILF1 was used to evaluate the role of constitutive receptor activity in this trans-inhibition across the BILF1-CXCR4 heteromer. Lysine 3.50 (Ballosteros-Weinstein numbering) is part of the EKT motif, which is the BILF1 variant of the highly conserved (E/D)RY motif present in class A GPCRs (45). Structural and mutational analysis of various class A GPCRs indicated that the (E/D)RY motif is involved in constraining the GPCR in an inactive conformation. This motif undergoes structural rearrangement upon receptor activation, allowing $Arg^{3.50}$ to directly interact with the G protein (1). Non-conservative mutations of $Arg^{3.50}$ impair G protein coupling of most GPCRs, which is generally accompanied with a loss of high affinity agonist binding, suggesting that $Arg^{3.50}$ mutants indeed adopt an inactive conformation (45). Previously it was shown that BILF1-$K^{3.50}$A did not constitutively signal to NF-κB (30). Co-expression of the constitutively inactive BILF1-$K^{3.50}$A with CXCR4 did not affect CXCL12-induced CXCR4 signaling as compared with cells expressing only the CXCR4 receptor. This suggests that propagation of the constitutively active conformation from BILF1 to the associated CXCR4 may indeed hamper CXCL12 binding to the latter. In addition, the absence of cross-inhibition within the BILF1-$K^{3.50}$A/CXCR4 heteromer reveals that other domains of BILF1 are not involved in inhibiting CXCR4 functioning as observed previously between the orphan GPR50 and the $MT_1$ melatonin receptor. The exceptionally long C-tail (>300 amino acids) of GPR50 inhibits protein recruitment to the GPR50/$MT_1$ heterodimer, or it may scavenge intracellular proteins that normally interact with $MT_1$; as a consequence melatonin binding and G protein coupling to the $MT_1$ protomer is inhibited (46). BILF1 and CXCR4 both couple predominantly to pertussis toxin-sensitive $G\alpha_{i/o}$ (Fig. 9) (25, 31, 32). In addition or alternatively to cross-conformational inhibition of CXCR4 within a BILF1/CXCR4 heteromer, the constitutive recruitment of $G\alpha_{i/o}$ proteins to BILF1 may hamper the precoupling of CXCR4 to this shared pool of $G\alpha_{i/o}$ proteins (Fig. 9*B*). Importantly,

Downloaded from www.jbc.org at Vrije Universiteit, Medical Library, on December 21, 2011

precoupled G proteins can allosterically modulate agonist binding to the extracellular site of GPCRs (47, 48). In fact, G proteins are strictly required for agonist binding to some GPCRs, including CXCR4 and various other chemokine receptors (Fig. 9*A*) (49–52). Supplementing BILF1/CXCR4-co-expressing HEK293T cells with additional $G\alpha_{i1}$ proteins overcame the BILF1-mediated inhibition of CXCR4 functioning, which, in combination with the inability of BILF1-$K^{3.50}$A to inhibit CXCR4, suggests that BILF1 attenuates CXCL12 binding to CXCR4 by constitutively scavenging $G\alpha_{i/o}$ proteins (Fig. 9*C*). On the other hand, binding of histamine to the $G\alpha_i$-coupled $H_4R$ was not affected by co-expression of BILF1, which is in concert with the recent observation that histamine binding to this receptor is G protein-independent (33). However, constitutive BILF1 signaling abolished histamine-induced $H_4R$ downstream signaling to CREB. Similar inhibitory cross-talk was recently observed between MOR and the constitutively active cannabinoid CB1 receptor, which both predominantly signal via $G\alpha_{i/o}$ proteins (17). DAMGO-induced MOR signaling was inhibited by co-expressed CB1 receptor in a ligand-independent manner. However, inhibiting constitutive CB1 receptor signaling to G proteins by co-incubation with an inverse agonist (*i.e.* SR141716A) or site-directed mutagenesis (*i.e.* CB1-$D^{3.49}$N) restored MOR-mediated ERK1/2 phosphorylation in response to DAMGO stimulation. As MOR and CB1 receptor are not assembled as heteromeric receptor complexes, cross-regulation of MOR signaling by the CB1 receptor is on a downstream intracellular level (17).

The chemokine receptor CXCR4 plays a key role in B cell homing and is expressed on most B cell populations, including plasma B cells (53). In addition, CXCR4 expression on tumor cells, including B cell lymphoma and EBV-associated nasopharyngeal carcinoma, allows these cells to metastasize toward CXCL12-secreting organs (54, 55). The EBV-encoded GPCR BILF1 forms hetero-oligomeric complexes with CXCR4 and inhibits CXCL12 binding to this receptor as a consequence of its constitutive activity. Attenuated migration of BILF1-expressing plasma B cells to CXCL12 gradients may be favorable for EBV, allowing these cells to home and/or remain at sites that are most optimal for viral replication and dissemination. Although cross-conformational inhibition of CXCR4 by BILF1 within an oligomeric assembly cannot be excluded, the current studies suggest that BILF1 inhibits the functioning of other $G_{i/o}$-coupled GPCRs by constitutive scavenging of a shared pool of $G_{i/o}$ proteins, thereby preventing other GPCRs from coupling to these G proteins (Fig. 9). Downstream cross-talk between BILF1 and other $G_{i/o}$-coupled receptors does not necessarily require or exclude hetero-oligomerization between these receptors. Nonetheless, hetero-oligomerization of this viral GPCR may well affect cellular receptor functioning on novel or distinct signaling pathways and/or affect receptor trafficking and mobility to, at, and from the cell surface, thereby contributing to viral dissemination and/or virus-induced pathologies.

## REFERENCES


1. Rosenbaum, D. M., Rasmussen, S. G., and Kobilka, B. K. (2009) *Nature* **459,** 356–363
2. Lagerström, M. C., and Schiöth, H. B. (2008) *Nat. Rev. Drug Discov.* **7,** 339–357
3. Gurevich, V. V., and Gurevich, E. V. (2008) *Trends Neurosci.* **31,** 74–81
4. Milligan, G. (2009) *Br. J. Pharmacol.* **158,** 5–14
5. Fotiadis, D., Jastrzebska, B., Philippsen, A., Müller, D. J., Palczewski, K., and Engel, A. (2006) *Curr. Opin. Struct. Biol.* **16,** 252–259
6. Banères, J. L., and Parello, J. (2003) *J. Mol. Biol.* **329,** 815–829
7. Damian, M., Martin, A., Mesnier, D., Pin, J. P., and Banères, J. L. (2006) *EMBO J.* **25,** 5693–5702
8. Kniazeff, J., Galvez, T., Labesse, G., and Pin, J. P. (2002) *J. Neurosci.* **22,** 7352–7361
9. Han, Y., Moreira, I. S., Urizar, E., Weinstein, H., and Javitch, J. A. (2009) *Nat. Chem. Biol.* **5,** 688–695
10. Vilardaga, J. P., Nikolaev, V. O., Lorenz, K., Ferrandon, S., Zhuang, Z., and Lohse, M. J. (2008) *Nat. Chem. Biol.* **4,** 126–131
11. Fotiadis, D., Liang, Y., Filipek, S., Saperstein, D. A., Engel, A., and Palczewski, K. (2003) *Nature* **421,** 127–128
12. Angers, S., Salahpour, A., Joly, E., Hilairet, S., Chelsky, D., Dennis, M., and Bouvier, M. (2000) *Proc. Natl. Acad. Sci. U.S.A.* **97,** 3684–3689
13. Whorton, M. R., Bokoch, M. P., Rasmussen, S. G., Huang, B., Zare, R. N., Kobilka, B., and Sunahara, R. K. (2007) *Proc. Natl. Acad. Sci. U.S.A.* **104,** 7682–7687
14. Whorton, M. R., Jastrzebska, B., Park, P. S., Fotiadis, D., Engel, A., Palczewski, K., and Sunahara, R. K. (2008) *J. Biol. Chem.* **283,** 4387–4394
15. White, J. F., Grodnitzky, J., Louis, J. M., Trinh, L. B., Shiloach, J., Gutierrez, J., Northup, J. K., and Grisshammer, R. (2007) *Proc. Natl. Acad. Sci. U.S.A.* **104,** 12199–12204
16. Hur, E. M., and Kim, K. T. (2002) *Cell. Signal.* **14,** 397–405
17. Canals, M., and Milligan, G. (2008) *J. Biol. Chem.* **283,** 11424–11434
18. Bakker, R. A., Casarosa, P., Timmerman, H., Smit, M. J., and Leurs, R. (2004) *J. Biol. Chem.* **279,** 5152–5161
19. Kelly, E., Bailey, C. P., and Henderson, G. (2008) *Br. J. Pharmacol.* **153,** Suppl. 1, S379–S388
20. Vischer, H. F., Vink, C., and Smit, M. J. (2006) *Curr. Top. Microbiol. Immunol.* **303,** 121–154
21. Vischer, H. F., Nijmeijer, S., Smit, M. J., and Leurs, R. (2008) *Biochem. Biophys. Res. Commun.* **377,** 93–97
22. Guo, W., Urizar, E., Kralikova, M., Mobarec, J. C., Shi, L., Filizola, M., and Javitch, J. A. (2008) *EMBO J.* **27,** 2293–2304
23. van Rijn, R. M., Chazot, P. L., Shenton, F. C., Sansuk, K., Bakker, R. A., and Leurs, R. (2006) *Mol. Pharmacol.* **70,** 604–615
24. Verzijl, D., Storelli, S., Scholten, D. J., Bosch, L., Reinhart, T. A., Streblow, D. N., Tensen, C. P., Fitzsimons, C. P., Zaman, G. J., Pease, J. E., de Esch, I. J., Smit, M. J., and Leurs, R. (2008) *J. Pharmacol. Exp. Ther.* **325,** 544–555
25. Beisser, P. S., Verzijl, D., Gruijthuijsen, Y. K., Beuken, E., Smit, M. J., Leurs, R., Bruggeman, C. A., and Vink, C. (2005) *J. Virol.* **79,** 441–449
26. Loening, A. M., Fenn, T. D., Wu, A. M., and Gambhir, S. S. (2006) *Protein Eng. Des. Sel.* **19,** 391–400
27. Kremers, G. J., Goedhart, J., van Munster, E. B., and Gadella, T. W., Jr. (2006) *Biochemistry* **45,** 6570–6580
28. Mercier, J. F., Salahpour, A., Angers, S., Breit, A., and Bouvier, M. (2002) *J. Biol. Chem.* **277,** 44925–44931
29. Ramsay, D., Kellett, E., McVey, M., Rees, S., and Milligan, G. (2002) *Biochem. J.* **365,** 429–440
30. Zuo, J., Currin, A., Griffin, B. D., Shannon-Lowe, C., Thomas, W. A., Ressing, M. E., Wiertz, E. J., and Rowe, M. (2009) *PLoS Pathog.* **5,** e1000255
31. Busillo, J. M., and Benovic, J. L. (2007) *Biochim. Biophys. Acta* **1768,** 952–963
32. Paulsen, S. J., Rosenkilde, M. M., Eugen-Olsen, J., and Kledal, T. N. (2005) *J. Virol.* **79,** 536–546
33. Schneider, E. H., Schnell, D., Papa, D., and Seifert, R. (2009) *Biochemistry* **48,** 1424–1438
34. Laichalk, L. L., and Thorley-Lawson, D. A. (2005) *J. Virol.* **79,** 1296–1307
35. Yuan, J., Cahir-McFarland, E., Zhao, B., and Kieff, E. (2006) *J. Virol.* **80,** 2548–2565
36. Maurel, D., Comps-Agrar, L., Brock, C., Rives, M. L., Bourrier, E., Ayoub, M. A., Bazin, H., Tinel, N., Durroux, T., Prezeau, L., Trinquet, E., and Pin,


Downloaded from www.jbc.org at Vrije Universiteit, Medical Library, on December 21, 2011

J. P. (2008) *Nat. Methods* **5,** 561–567
37. Park, P. S., and Wells, J. W. (2004) *J. Neurochem.* **90,** 537–548
38. Gandia, J., Galino, J., Amaral, O. B., Soriano, A., Lluís, C., Franco, R., and Ciruela, F. (2008) *FEBS Lett.* **582,** 2979–2984
39. Lopez-Gimenez, J. F., Canals, M., Pediani, J. D., and Milligan, G. (2007) *Mol. Pharmacol.* **71,** 1015–1029
40. Carriba, P., Navarro, G., Ciruela, F., Ferré, S., Casadó, V., Agnati, L., Cortés, A., Mallol, J., Fuxe, K., Canela, E. I., Lluís, C., and Franco, R. (2008) *Nat. Methods* **5,** 727–733
41. Sohy, D., Yano, H., de Nadai, P., Urizar, E., Guillabert, A., Javitch, J. A., Parmentier, M., and Springael, J. Y. (2009) *J. Biol. Chem.* **284,** 31270–31279
42. Sohy, D., Parmentier, M., and Springael, J. Y. (2007) *J. Biol. Chem.* **282,** 30062–30069
43. Levoye, A., Balabanian, K., Baleux, F., Bachelerie, F., and Lagane, B. (2009) *Blood* **113,** 6085–6093
44. Jordan, B. A., Gomes, I., Rios, C., Filipovska, J., and Devi, L. A. (2003) *Mol. Pharmacol.* **64,** 1317–1324
45. Rovati, G. E., Capra, V., and Neubig, R. R. (2007) *Mol. Pharmacol.* **71,** 959–964
46. Levoye, A., Dam, J., Ayoub, M. A., Guillaume, J. L., Couturier, C., Delagrange, P., and Jockers, R. (2006) *EMBO J.* **25,** 3012–3023
47. Chabre, M., Deterre, P., and Antonny, B. (2009) *Trends Pharmacol. Sci.* **30,** 182–187
48. Christopoulos, A., and Kenakin, T. (2002) *Pharmacol. Rev.* **54,** 323–374
49. Bouvier, M., Ménard, L., Dennis, M., and Marullo, S. (1998) *Curr. Opin. Biotechnol.* **9,** 522–527
50. Gupta, S. K., Pillarisetti, K., Thomas, R. A., and Aiyar, N. (2001) *Immunol. Lett.* **78,** 29–34
51. Maeda, Y., Kuroki, R., Haase, W., Michel, H., and Reiländer, H. (2004) *Eur. J. Biochem.* **271,** 1677–1689
52. Springael, J. Y., Le Minh, P. N., Urizar, E., Costagliola, S., Vassart, G., and Parmentier, M. (2006) *Mol. Pharmacol.* **69,** 1652–1661
53. Kunkel, E. J., and Butcher, E. C. (2003) *Nat. Rev. Immunol.* **3,** 822–829
54. Hu, J., Deng, X., Bian, X., Li, G., Tong, Y., Li, Y., Wang, Q., Xin, R., He, X., Zhou, G., Xie, P., Li, Y., Wang, J. M., and Cao, Y. (2005) *Clin. Cancer Res.* **11,** 4658–4665
55. Piovan, E., Tosello, V., Indraccolo, S., Cabrelle, A., Baesso, I., Trentin, L., Zamarchi, R., Tamamura, H., Fujii, N., Semenzato, G., Chieco-Bianchi, L., and Amadori, A. (2005) *Blood* **105,** 931–939

Downloaded from www.jbc.org at Vrije Universiteit, Medical Library, on December 21, 2011